Environmental Science & Technology

Article

pubs.acs.org/est

Multiple Sulfur Isotope Constraints on Sources and Formation Processes of Sulfate in Beijing $PM_{2.5}$ Aerosol

Xiaokun Han,[†] Qingjun Guo,[*,†,‡] Harald Strauss,[§] Congqiang Liu,[∥] Jian Hu,[∥] Zhaobing Guo,[⊥] Rongfei Wei,[†] Marc Peters,[†] Liyan Tian,[†] and Jing Kong[†]

[†]Center for Environmental Remediation, Institute of Geographic Sciences and Natural Resources Research, Chinese Academy of Sciences, 11A Datun Road, Chaoyang, Beijing 100101, China

[‡]College of Resources and Environment, University of Chinese Academy of Sciences, Beijing 100049, China

[§]Institut für Geologie und Paläontologie, Westfälische Wilhelms-Universität Münster, Corrensstrasse 24, 48149 Münster, Germany

[∥]State Key Laboratory of Environmental Geochemistry, Institute of Geochemistry, Chinese Academy of Sciences, Guiyang Guizhou 550002, China

[⊥]School of Environmental Science and Engineering, Nanjing University of Information Science and Technology, Nanjing 210044, China

Supporting Information

ABSTRACT: Recently air pollution is seriously threatening the health of millions of people in China. The multiple sulfur isotopic composition of sulfate in $PM_{2.5}$ samples collected in Beijing is used to better constrain potential sources and formation processes of sulfate aerosol. The $\Delta^{33}S$ values of sulfate in $PM_{2.5}$ show a pronounced seasonality with positive values in spring, summer and autumn and negative values in winter. Positive $\Delta^{33}S$ anomalies are interpreted to result from SO_2 photolysis with self-shielding, and may reflect air mass transport between the troposphere and the stratosphere. The negative $\Delta^{33}S$ signature ($-0.300‰ < \Delta^{33}S < 0‰$) in winter is possibly related to incomplete combustion of coal in residential stoves during the heating season, implying that sulfur dioxide released from residential stoves in more rural areas is an important contributor to atmospheric sulfate. However, negative $\Delta^{33}S$ anomalies ($-0.664‰ < \Delta^{33}S \leftarrow 0.300‰$) in winter and positive $\Delta^{33}S$ anomalies ($0.300‰ < \Delta^{33}S < 0.480‰$) in spring, summer, and autumn suggest sulfur isotopic equilibrium on an annual time frame, which may provide an implication for the absence of mass-independent fractionation of sulfur isotopes (S-MIF) in younger sediments. Results obtained here reveal that reducing the usage of coal and improving the heating system in rural areas will be important for efficiently decreasing the emissions of sulfur in China and beyond.

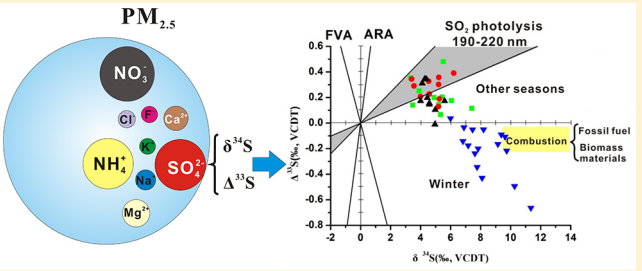

1. INTRODUCTION

Air pollution by particulate matter is a serious problem in China.[1,2] In recent years, severe haze events with extremely high mass concentrations of particulate matter have frequently occurred in numerous cities in China, including Beijing.[2−5] Airborne particulate matter, especially $PM_{2.5}$ aerosol (aerodynamic diameter ≤ 2.5 μm), has adverse impacts on human health, visibility and climate change.[2,6,7] Aerosols can be directly released from natural and anthropogenic sources (primary aerosol) or formed by gas-to-particle conversion (secondary aerosol).[1] Previous studies show that major chemical components of $PM_{2.5}$ in China are organic matter, sulfate, nitrate, ammonium, elemental carbon and chloride, etc.[1,2,8] Coal combustion, biomass burning, industrial emission, vehicle exhaust, and resuspended dust are considered to be the major sources of $PM_{2.5}$ in China.[1,2,4,5] Recent studies suggest that severe haze events in China were mainly controlled by secondary aerosols, which were composed of approximately equal amounts of secondary inorganic aerosols and secondary organic aerosols.[2,8] At present, the formation mechanisms resulting in haze events in China remain uncertain.

Sulfate, as one of the major chemical species in $PM_{2.5}$, plays an important role in environmental chemistry and climate change.[7,9] Investigations of multiple sulfur isotopic compositions of sulfate in $PM_{2.5}$ will provide crucial information about its sources and formation processes.

Traditional sulfur isotopes ($\delta^{34}S$) are useful in distinguishing different sulfur sources and estimating the relative contribution by these sources because different sources display different $\delta^{34}S$ values.[10−15] Numerous studies have been conducted in China,[10,12,13] Japan,[14,15] Europe,[16] and Antarctica[17] to identify atmospheric sulfate sources using sulfur isotopes. Apart from source identification and source apportionment, sulfur isotopes

Received: January 16, 2017
Revised: May 29, 2017
Accepted: June 12, 2017
Published: June 12, 2017

DOI: 10.1021/acs.est.7b00280
Environ. Sci. Technol. 2017, 51, 7794−7803

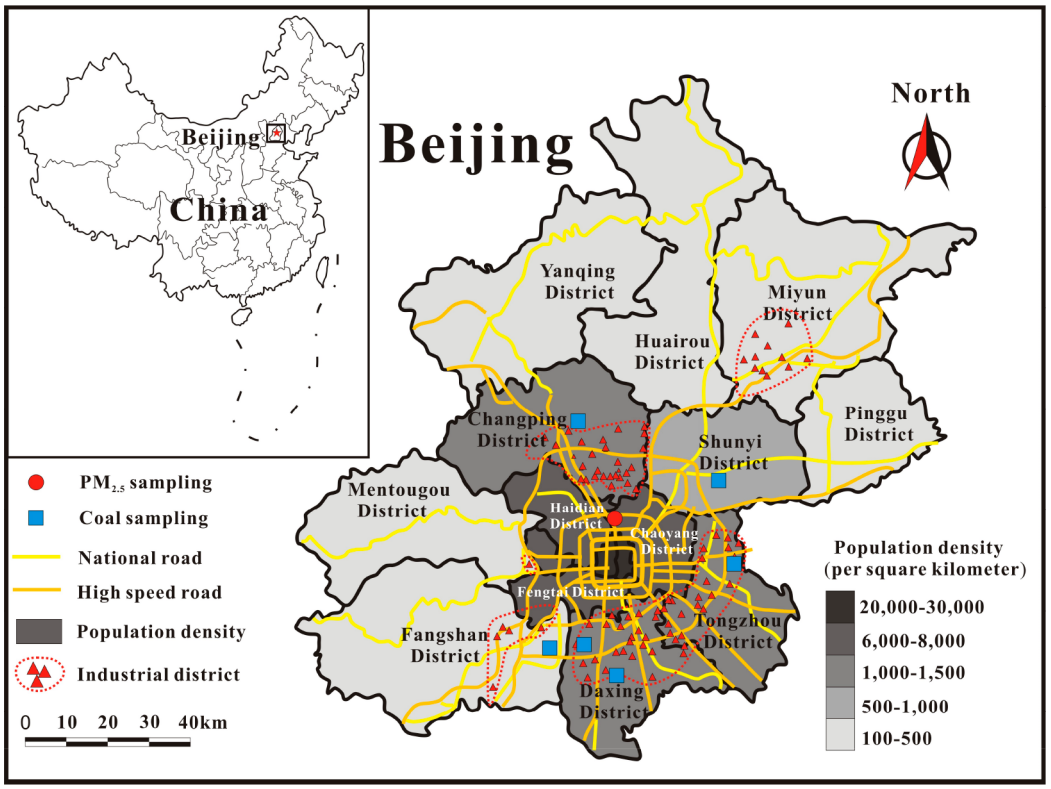

Figure 1. Location of sampling site in Beijing, China. Modified from Guo, Q.; Strauss, H.; Chen, T.B.; Zhu, G.; Yang, J.; Yang, J.; Lei, M.; Zhou, X.; Peters, M.; Xie, Y.; Zhang, H.; Wei, R.; Wang, C. Tracing the source of Beijing soil organic carbon: a carbon isotope approach. Environ. Pollut. 2013, 176, 208−214.[63] Copyright 2013 Elsevier. The data of population density are from Meng and Tang (2010).[64] The sampling site for $PM_{2.5}$ is located on the building roof (around 24 m above ground level) of the Institute of Geographic Sciences and Natural Resources Research, Chinese Academy of Sciences in Beijing, which is between the north fourth and fifth ring road.

allow for investigating the oxidation processes of SO_2 in the atmosphere because of distinctive isotopic fractionation associated with different oxidation reactions.[11,18]

Multiple sulfur isotopes have been used to trace the evolution of Earth's atmosphere,[19−21] to document large volcanic eruptions in the past,[22−24] and to identify sources, formation processes and the transport of sulfate in the modern atmosphere.[25−27] Mass-independent fractionation of sulfur isotopes (S-MIF) recorded in sedimentary rocks older than 2.45 Ga, and the loss of this signal in younger rocks, is thought to reflect a dramatic change in atmospheric oxygen concentration, that is, from an anoxic to an oxic atmosphere.[19,20,28] The S-MIF signal in >2.45 Ga old rocks has been ascribed to photochemistry in an oxygen-poor atmosphere.[19,20,29] Laboratory experiments have shown that UV irradiation of SO_2 in the 190−220 nm region can produce large S-MIF signals.[29−31] In our present oxic atmosphere, SO_2 photolysis can not occur below an altitude of 20km.[32] SO_2 from volcanic eruptions can reach an altitude above 20km and experience UV photolysis in the 190−210 nm region.[22] Resulting S-MIF signals have been preserved in polar ice cores, providing information about the dynamics of volcanic emissions in the past.[22,23] Recently, mass independent sulfur isotopic fractionation has been observed in modern non-volcanic sulfate aerosols, which implies the mass transport of sulfate/SO_x between troposphere and stratosphere.[25−27] For example, S-MIF signals were measured in recent snow layers at the South Pole. They are related with super El Niño Southern Oscillation (ENSO) during 1997−1998, suggesting that the sulfur isotope anomalies may result from changes in dynamics of the upper troposphere and lower stratosphere.[27]

In this study, we extend our previous research on sulfate aerosols[13] toward the minor sulfur isotope ^{33}S of sulfate in $PM_{2.5}$ samples collected in Beijing to better understand the sources and formation processes of sulfate, which can be crucial for improving the air quality in Chinese megacities. By combining meteorological data and concentrations of water-soluble ions in $PM_{2.5}$, the seasonality in multiple sulfur isotopes will be discussed.

2. MATERIALS AND METHODS

2.1. Sampling. Beijing is located on the northern border of the North China Plain, about 150km northwest of the Bohai Sea, and it is surrounded by the Yanshan Mountains in the west, north, and northeast. Beijing experiences a typical continental monsoon climate with four distinct seasons, that is, high-speed winds and low rain in spring, high temperature and frequent rain in summer, northwest winds and sunny days in autumn, and dry and cold air in winter. The sampling site is located on the building roof (around 24 m above ground level) of the Institute of Geographic Sciences and Natural Resources Research, Chinese Academy of Sciences in Beijing (Figure 1), which is between the north fourth and fifth ring road. No large buildings surround the sampling site due to its location at the western margin of Olympic Forest Park, a large urban park area.

Sampling of $PM_{2.5}$ aerosol was performed during four seasons between July 5, 2015 and April 29, 2016 (n = 46). $PM_{2.5}$ samples were collected for 24 h on precombusted (450 °C for 6 h) quartz fiber filters (20 cm × 25 cm, Munktell,

DOI: 10.1021/acs.est.7b00280
Environ. Sci. Technol. 2017, 51, 7794−7803

Sweden) using a high-volume air sampler (TH-1000H, Tianhong Wuhan) at a flow rate of 1.05 m^3 min^{-1}. After sampling, the filters were stored in a freezer at −20 °C prior to analysis.

Meteorological data for the sampling periods were obtained from the National Meteorological Information Center (http://data.cma.cn/site/index.html, Figure S1), and daily mean values of air temperature, air humidity, atmospheric pressure, and wind speed were calculated based on observational data for 2.00 a.m., 8.00 a.m., 14.00 p.m., and 20.00 p.m. The detection limits for precipitation, air temperature, air humidity, atmospheric pressure and wind speed are 0.1 mm, 0.1 °C, 1%, 0.1 hPa, and 0.1 m/s, respectively.

In addition, 14 coal samples were collected from rural residences in the Beijing suburbs. Sampling points for coal were selected from different districts surrounding the Beijing urban area, that is, Changping district, Shunyi district, Tongzhou district, Daxing district, and Fangshan district (Figure 1).

2.2. Chemical and Isotopic Measurements. Half of each filter was cut into pieces and soaked in 200 mL of Milli-Q water for 30 min added by ultrasonification.[11] The filter was kept in the water for 12 h to thoroughly extract the water-soluble ions. The quartz filter fibers were then removed through filtration using 0.45 μm Millipore filters. An aliquot of 10 mL withdrawn from the filtered solution was used for concentration measurements. The remaining solution was acidified with HCl to a pH to <2 and heated up to boiling. Subsequently, 25 mL of 8.5% $BaCl_2$ solution was added into the solution to quantitatively precipitate barium sulfate. The solution containing barium sulfate was kept at 80 °C for 3 h. Thereafter, the barium sulfate precipitates were collected on 0.22 μm acetate Millipore filter, rinsed with ∼150 mL Milli-Q water,[26] and dried in an oven at 45 °C for 48 h. Blank samples were analyzed accordingly.

Around 9 mg of barium sulfate was converted to H_2S by adding a mixture of H_3PO_2, HI, and HCl solution.[33,34] H_2S was carried by a stream of N_2 through a distilled water trap, collected subsequently in an acetic acid zinc acetate solution (3.5%). Resulting ZnS was converted to Ag_2S by adding 10 mL of 0.1 mol/L $AgNO_3$. The Ag_2S precipitates were filtered (0.45 μm), thoroughly washed with ∼5 mL of 5% NH_4OH and ∼250 mL of Milli-Q water, and dried in an oven at 45 °C for 48 h at the Institute of Geographic Sciences and Natural Resources Research, Chinese Academy of Sciences.

The concentrations of water-soluble ions (SO_4^{2-}, NO_3^-, Cl^-, F^-, NH_4^+, Na^+, K^+, Ca^{2+}, and Mg^{2+}) were analyzed via ion chromatography (Dionex ICS900) at the Institute of Geographic Sciences and Natural Resources Research, Chinese Academy of Sciences, which consists of a separation column (Dionex IonPac AS23 for anion and CS12A for cation), a guard column (Dionex IonPac AG23 for anion and CG12A for cation), a self-regenerating micromembrane suppressor (Dionex AERS 500 for anion and Dionex CERS500 for cation) and an electrical conductivity detector (Dionex IonPac DS5). The eluent for anions consists of 0.8 mM $NaHCO_3$ and 4.5 mM Na_2CO_3; 20 mM methansulfonic acid (MSA) was used as the eluent for cations. The recovery for each ion was between 80% and 120%. The relative standard deviation of repetitive measurements was less than 5% for each ion. The detection limits vary from 0.03 to 0.07 $\mu g/m^3$ for anions and from 0.01 to 0.04 $\mu g/m^3$ for cations. Blank values were used for calibration.

Around 3 mg of Ag_2S were packaged in aceton cleaned aluminum foil and loaded into nickel reactors. Ag_2S was converted to SF_6 via fluorination with a 5-fold excess of fluorine gas at 300 °C for 12 h. Resulting SF_6 was purified cryogenically in a cold trap at −115 °C to −119 °C, followed by gas chromatography consisting of a Molecular Sieve 5A column (1/8-in. diameter) and a Haysep-Q column (1/8-in. diameter). The flow rate of helium gas was 20 mL/min. Finally, the SF_6 gas was frozen into a liquid-nitrogen cold trap and subsequently transferred to a ThermoFinnigan MAT 253 equipped with a dual inlet system at the Institut für Geologie and Paläontologie, Westfälische Wilhelms-Universität Münster. Results are expressed as[35,36]

$$\delta^{34}S = [(^{34}S/^{32}S)_{sample}/(^{34}S/^{32}S)_{reference} - 1] \times 1000 \quad (1)$$

$$\Delta^{33}S = \delta^{33}S - [(\delta^{34}S/1000 + 1)^{0.515} - 1] \times 1000 \quad (2)$$

where $\Delta^{33}S$ represents the deviation of measured $\delta^{33}S$ and $\delta^{34}S$ from the theoretical mass fractionation line for $\delta^{33}S$ and $\delta^{34}S$. Mass-independent fractionation of sulfur isotopes (S-MIF) means that measured isotope compositions ($\delta^{33}S$ and $\delta^{34}S$) do not lie on the mass fractionation line with a slope of 0.515. When $|\Delta^{33}S|>0.2$ ‰ and the range of $\delta^{34}S$ is less than 10 ‰, it is generally believed that the effect of mass independent fractionation occurs.

On the basis of long-term measurements of standard material IAEA-S-1, uncertainties (1σ) for $\delta^{34}S$ and $\Delta^{33}S$ values are within ±0.2 ‰ and ±0.01 ‰, respectively.

Dried coal samples were pulverized to less than 200 mesh. Sulfur in coal samples was extracted using the Eschka method. The Eschka reagent was obtained by a mixture of MgO and Na_2CO_3 at a mass ratio of 2:1. One g of coal powder was mixed uniformly with 3 g of Eschka reagent. The mixture was placed into a ceramic crucible and then covered by 1 g of Eschka reagent. Next, the ceramic crucible was placed into the muffle furnace and heated up to 850 °C. The incinerated mixture was dissolved in 200 mL of Milli-Q water. The filtered solution was acidified with HCl to a pH to <2 and heated up to boiling. Subsequently, 25 mL of 8.5% $BaCl_2$ solution was added into the solution to quantitatively precipitate barium sulfate.

The sulfur isotope ($\delta^{34}S$) measurements for coal samples were performed using an Elemental Analyzer (EA) coupled to a Delta V Advantage Isotope Ratio Mass Spectrometer (IRMS) at the Institute of Geographic Sciences and Natural Resources Research, Chinese Academy of Sciences. The results are reported in the standard delta notation relative to the Vienna Canyon Diablo Troilite standard (V-CDT). The $\delta^{34}S$ measurements were calibrated against the reference materials NBS127 ($\delta^{34}S$ = 21.17 ‰) and IAEA-SO-5 ($\delta^{34}S$ = 0.5 ‰). The reproducibility of the measurements was better than ±0.2 ‰.

2.3. Back Trajectory Analysis. The impact of regional air mass transport on the $PM_{2.5}$ composition was analyzed using hybrid single-particle Lagrangian integrated trajectory (HYSPLIT) model.[37] Back trajectories (48 h) at 50, 200, and 500 m arrival height above ground were computed every 6 h, respectively.

3. RESULTS

3.1. Water-Soluble Inorganic Ions. The concentrations of water-soluble inorganic ions (WSII) in the $PM_{2.5}$ aerosols are listed in Table S1. The concentrations of WSII are in the order of NO_3^- > SO_4^{2-} > NH_4^+> Cl^- > Ca^{2+} > K^+ > Na^+ > F^- > Mg^{2+}. NO_3^-, SO_4^{2-}, and NH_4^+ are the predominant ions, on average, collectively accounting for ∼85% (nequiv %) of WSII.

DOI: 10.1021/acs.est.7b00280
Environ. Sci. Technol. 2017, 51, 7794−7803

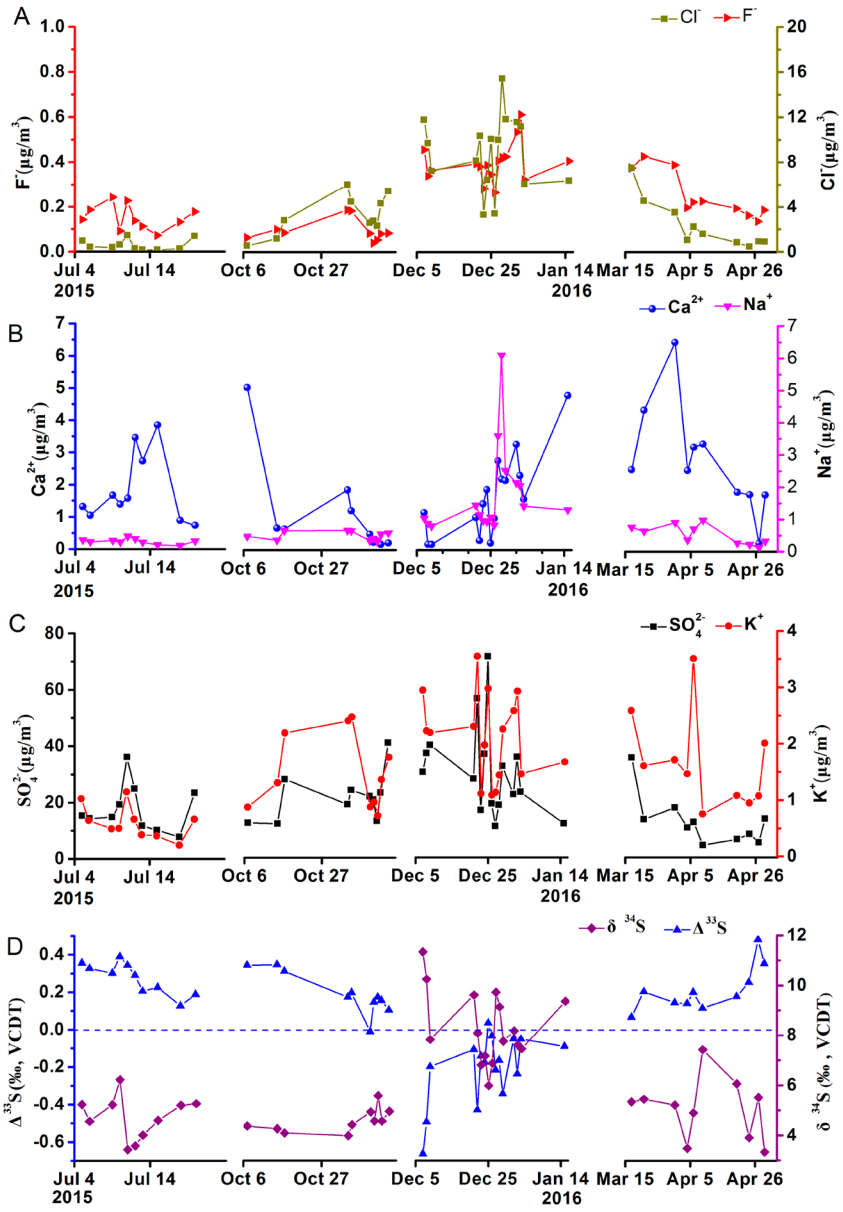

Figure 2. Variations in F^-, Cl^-, SO_4^{2-}, Ca^{2+}, Na^+, and K^+ concentrations and multiple sulfur isotopic compositions of sulfate in $PM_{2.5}$ during individual sampling periods. (A) F^- and Cl^- concentrations; (B) Ca^{2+} and Na^+ concentrations; (C) SO_4^{2-} and K^+ concentrations; (D) $\delta^{34}S$ and $\Delta^{33}S$.

The nitrate, sulfate and ammonium equivalent concentrations range from 72 to 1552 nequiv/m^3 (mean = 470 ± 313 nequiv/m^3, n = 46), from 90 to 1486 nequiv/m^3 (mean = 459 ± 280 nequiv/m^3, n = 46), and from 131 to 2430 nequiv/m^3 (mean = 872 ± 500 nequiv/m^3, n = 46), respectively. The equivalent concentration ratio of $NH_4^+/[SO_4^{2-}+NO_3^-]$ varies from 0.69 to 1.36 with a mean value of 0.94 ± 0.14(n = 46). Cl^- equivalent concentration shows an obvious seasonality, that is, high in winter (mean = 252 ± 93 nequiv/m^3, n = 16) and low in summer (mean = 15 ± 14 nequiv/m^3, n = 10). The average equivalent concentrations of K^+, Na^+, F^-, and Mg^{2+} are lower than 50 nequiv/m^3.

3.2. Multiple Sulfur Isotopes. Multiple sulfur isotopic compositions of sulfate ($\delta^{34}S$ and $\Delta^{33}S$) in Beijing $PM_{2.5}$ are listed in Table S1 and shown in Figure 2. $\delta^{34}S$ values vary from 3.3 ‰ to 11.4 ‰ (mean = 6.0 ± 2.0 ‰, n = 46) and exhibit a significant seasonality, that is, low values in summer and high values in winter. During spring, summer, autumn and winter, the mean values of $\delta^{34}S$ in sulfate are 5.1 ± 1.2 ‰ (n = 10), 4.7 ± 0.9 ‰ (n = 10), 4.6 ± 0.5 ‰ (n = 10), and 8.3 ± 1.5 ‰ (n = 16), respectively. $\Delta^{33}S$ values of sulfate in $PM_{2.5}$ range from −0.664 ‰ to 0.480 ‰ (mean = 0.075 ± 0.253 ‰), and also show a pronounced seasonality. During spring, summer and autumn, $\Delta^{33}S$ values are clearly positive around a mean value of 0.227 ± 0.110 ‰ (n = 30). In contrast, during winter negative $\Delta^{33}S$ values ranging from −0.664 ‰ to 0.035 ‰ (mean = −0.211 ± 0.188 ‰, n = 18) were measured for $PM_{2.5}$. To the best of our knowledge, this is the first report of negative $\Delta^{33}S$ signatures for sulfate aerosol in the modern atmosphere.

4. DISCUSSION

4.1. $\delta^{34}S$ in $PM_{2.5}$ Implying Atmospheric Sulfur Sources. Sulfur isotopes from sulfate aerosols have been used to distinguish anthropogenic and natural sources of

DOI: 10.1021/acs.est.7b00280
Environ. Sci. Technol. 2017, 51, 7794−7803

atmospheric sulfur based on their distinct $\delta^{34}S$ values.[10,11,13,15] The $\delta^{34}S$ values, plotted against sulfate concentration (Figure 3), indicate that sulfate in $PM_{2.5}$ is reflecting a complex mixture

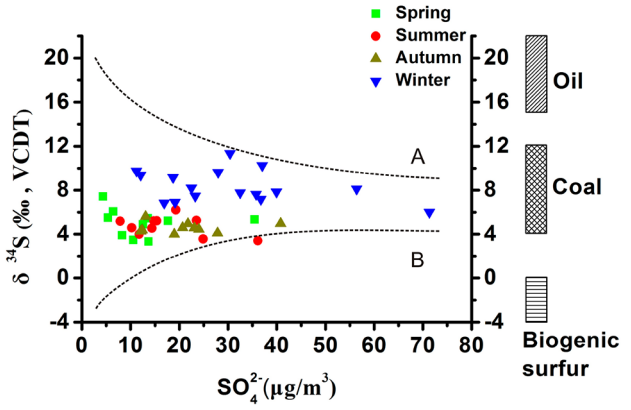

Figure 3. $\delta^{34}S$ values and sulfate concentration in Beijing $PM_{2.5}$ compared to a ternary mixing model. Considering the regional transport of $PM_{2.5}$, the mean $\delta^{34}S$ value (+6.6‰) of coal in North China is used. Curve A shows a mixture between sulfur in oil ($\delta^{34}S$ value = 20.5‰) and coal ($\delta^{34}S$ value = 6.6‰). Curve B show a mixture between biogenic sulfur ($\delta^{34}S$ value = −10‰) and sulfur in coal ($\delta^{34}S$ value = 6.6‰).

of different sulfur sources having high and low $\delta^{34}S$ values. On the basis of the data from Smithsonian database of global volcanic eruptions (www.volcano.si.edu), no volcanic activities occurred in China, Mongolia, North Korea, and South Korea during 2014−2016. Consequently, volcanic SO_2 as a source of atmospheric sulfur in Beijing can be ruled out. A contribution of sea-salt sulfate is also rather unlikely because of the low concentration of Na^+ (0.41 ± 0.23 $\mu g/m^3$, n = 30) in spring, summer and autumn. The concentration of Na^+ is higher in winter (1.71 ± 1.38 $\mu g/m^3$, n = 16). Moreover, back trajectory analyses show that the air masses in winter originate from northwest and south of Beijing (Figure S2), which supports the assumption of a very low to negligible contribution of sea-salt sulfate. The higher Na^+ concentration in winter was likely caused by the enhanced contribution from coal combustion and the lower boundary layer height.

Sulfate in aerosols can be derived from a terrigenous source. Ca^{2+} has been considered as an indicator of this.[38] The contribution of sulfate from a terrigenous source (f_{ts}) can be estimated by the equation

$$f_{ts} = (SO_4^{2-}/Ca^{2+})_{soil}/(SO_4^{2-}/Ca^{2+})_{aerosol} \quad (3)$$

where the ratio of $(SO_4^{2-}/Ca^{2+})_{soil}$ in China ranges from 0.29 to 0.43.[39,40] Results indicate that the average contribution of sulfate from a terrigenous source varies from 3.83 ± 4.40% to 5.69 ± 6.52%. However, Ca^{2+} in $PM_{2.5}$ could originate from fly ash emitted from coal combustion followed by solubilization during atmospheric aging process, suggesting that Ca^{2+} in $PM_{2.5}$ does not all come from a terrigenous source. Therefore, the estimation of terrigenous contribution to sulfate in $PM_{2.5}$ is higher than the actual contribution, which implies that sulfate from soil or mineral dusts account for a rather small proportion of sulfate in Beijing $PM_{2.5}$. This is further confirmed by a weak correlation between SO_4^{2-} and Ca^{2+} (r = −0.37, Table 1).

SO_2 can be emitted from oil combustion. It was reported that the sulfur content and its $\delta^{34}S$ values in oil used in North China varied from 0.1% to 0.6% and from 13.7% and 24.2 ‰, respectively.[41] In North China, hundreds of million tons of petroleum products are being consumed by a wide range of industries. Consequently, oil combustion can be identified as a sulfur source having a relatively high $\delta^{34}S$ value.

Biogenic sulfur from soils and wetlands, which is a natural source of atmospheric sulfur, has a low $\delta^{34}S$ value of −10 ‰ to −2 ‰.[42−44] However, the mean values of $\delta^{34}S$ in sulfate of $PM_{2.5}$ for spring, summer, autumn, and winter are 5.1 ± 1.2 ‰ (n = 10), 4.7 ± 0.9 ‰ (n = 10), 4.6 ± 0.5 ‰ (n = 10), and 8.3 ± 1.5 ‰ (n = 16), respectively. These values for $PM_{2.5}$ are distinctly different from values for sulfur from oil and biogenic origin, suggesting sulfate in $PM_{2.5}$ is a mixture of different sulfur sources.

Previous reports indicated that sulfur emissions from coal combustion make a significant contribution to the atmospheric sulfur pool in China.[10,13,26] Sulfur isotopic fractionation occurs during the process of coal combustion.[45] The released SO_2 is depleted in ^{34}S while the SO_4^{2-} in the solid ash is enriched in ^{34}S relative to the total sulfur in the coal.[45] Despite of these, Mukai et al. observed that the mean $\delta^{34}S$ values of atmospheric sulfur in China were close to the sulfur isotope compositions of the coal used in the respective area.[10] Furthermore, Novák et al. reported that the increasing coal consumption in winter lead to a change in $\delta^{34}S$ of SO_2 in atmosphere.[46] In consideration of coal as a dominant energy source in China, a direct comparison

Table 1. Correlation Coefficients for Water-Soluble Ions and Stable Isotopes of $PM_{2.5}$ in Beijing[a]

	Na^+	NH_4^+	K^+	Mg^{2+}	Ca^{2+}	F^-	Cl^-	NO_3^-	SO_4^{2-}	$\delta^{34}S$	$\delta^{18}O$	$\Delta^{33}S$
Na^+	1.00											
NH_4^+	0.20	1.00										
K^+	0.27	0.83**	1.00									
Mg^{2+}	0.44**	0.04	0.26	1.00								
Ca^{2+}	0.16	−0.31*	−0.06	0.70**	1.00							
F^-	0.61**	0.48**	0.60**	0.65**	0.27	1.00						
Cl^-	0.77**	0.67**	0.68**	0.38**	−0.06	0.80**	1.00					
NO_3^-	0.07	0.87**	0.72**	0.08	−0.19	0.33*	0.45**	1.00				
SO_4^{2-}	0.13	0.89**	0.63**	−0.05	−0.37*	0.38*	0.57**	0.65**	1.00			
$\delta^{34}S$	0.60**	0.29*	0.37*	0.26	−0.03	0.71**	0.76**	0.05	0.25	1.00		
$\delta^{18}O$	−0.21	−0.25	−0.31*	−0.17	−0.06	−0.47**	−0.30*	−0.25	−0.18	−0.32*	1.00	
$\Delta^{33}S$	−0.51**	−0.51**	−0.53**	−0.22	0.11	−0.70**	−0.81**	−0.21	−0.48**	−0.84**	0.26	1.00

[a]*Significant at 0.05 level. **Significant at 0.01 level. n = 46.

DOI: 10.1021/acs.est.7b00280
Environ. Sci. Technol. 2017, 51, 7794−7803

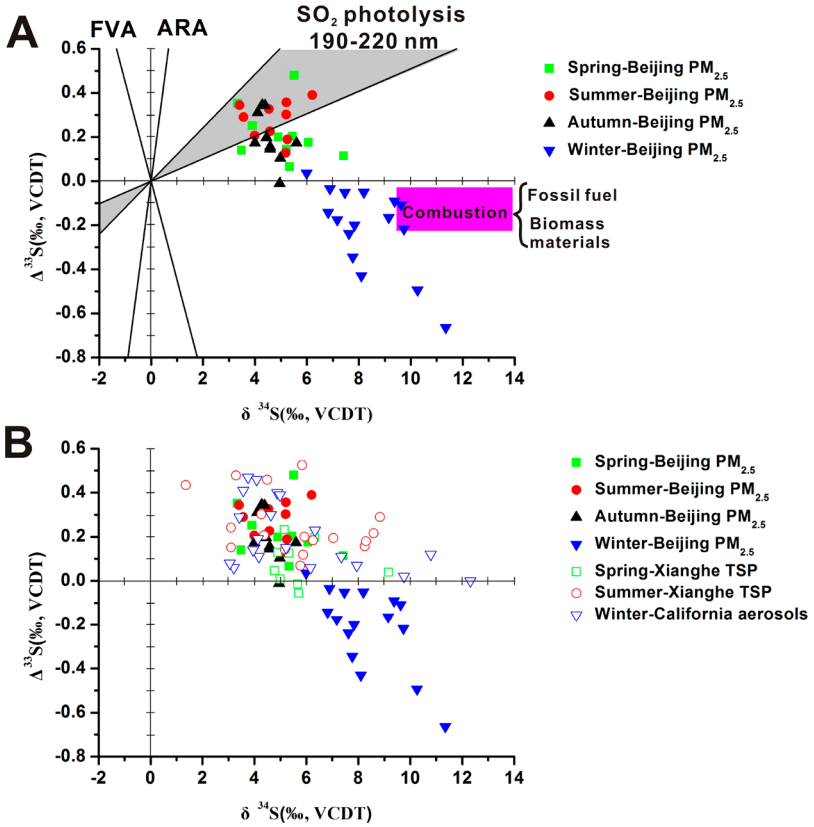

Figure 4. (A) Relation between $\delta^{34}S$ and $\Delta^{33}S$ for sulfate in Beijing $PM_{2.5}$ during sampling and (B) their comparison with aerosols collected from Xianghe, Hebei Province, China[26] and from Bakersfield, California, America.[25] ARA represents Archean Reference Array based on the data from Neoarchean and Paleoarchean rocks in Australia and Africa.[44] FVA represents felsic volcanic array reported by Philippot et al.[24] Gray field represents experiment data from SO_2 photolysis in 190−220 nm region (Xenon arc lamp).[44] Aubergine field represents experiment data from combustion of fossil fuel and biomass materials.[51] Limited experimental data display that $\Delta^{33}S$ values of sulfate from combustion of fossil fuel and (modern) biomass exhibit no significant differences.

between $\delta^{34}S$ values of sulfate in $PM_{2.5}$ and those of coals in a local region appears most logical.

Here, the mean $\delta^{34}S$ value of sulfate in $PM_{2.5}$ (6.0 ± 2.0 ‰, n = 46) is close to those of coals used in North China (mean = +6.6 ‰).[41,45] Considering sulfate from oil and biogenic origin, it suggests that coal combustion is one of the major sources of sulfate in $PM_{2.5}$ aerosols in Beijing (Figure 3). The oxygen isotopic composition of sulfate can reflect oxidation processes.[11] The $\delta^{18}O$ value of primary sulfate (~+40‰) formed in the emission source is much heavier than that of secondary sulfate (~−10−+20‰) formed by SO_2 oxidation.[47] The mean $\delta^{18}O$ value of sulfate in $PM_{2.5}$ is 12.8 ± 4.4 ‰ (n = 46, unpublished results). The proportion of primary and secondary sulfate in $PM_{2.5}$ can be estimated based on equations developed by Holt(1991)[47] and the mean $\delta^{18}O$ value of precipitation in Beijing (−7.3‰).[48] It shows that most of the sulfate in $PM_{2.5}$ is formed through oxidation of SO_2, which is consistent with the results reported by Guo et al.[49] Moreover, the mean $\delta^{34}S$ value of coal used for heating in the Beijing suburbs (8.0 ± 3.0 ‰, n = 14), determined in this study, agrees well with the mean value of $\delta^{34}S$ in sulfate of Beijing $PM_{2.5}$ in winter (8.3 ± 1.5 ‰, n = 16). This indicates that, in winter, the contribution of secondary sulfate from coal combustion is considerable to sulfate in $PM_{2.5}$. This has been confirmed by our recent study, which shows that the contribution of coal combustion during the winter season in Beijing can account for up to 80.9% of sulfate in total suspended particulates (TSP).[13] In addition, the mean $\delta^{34}S$ value of sulfate in TSP (6.6 ± 1.8 ‰, n = 70)[13] is similar to that in $PM_{2.5}$ (6.0 ± 2.0 ‰, n = 46), suggesting that sources of sulfate were basically identical to TSP and $PM_{2.5}$.

4.2. $\Delta^{33}S$ Signatures of Sulfate in $PM_{2.5}$. Positive $\Delta^{33}S$ values as high as 0.480‰ were measured in sulfate of $PM_{2.5}$ for spring, summer and autumn, while negative $\Delta^{33}S$ values as large as −0.664‰ were recorded in winter (Figure 2). Obviously, some samples reflect truly mass independent fractionation of sulfur isotopes (S-MIF). In the $\delta^{34}S$−$\Delta^{33}S$ diagram (Figure 4A), the sulfur isotopic compositions of $PM_{2.5}$ display a negative slope ($\delta^{34}S$−$\Delta^{33}S$ slope = −0.10) different from the Archean reference array (ARA) ($\delta^{34}S$−$\Delta^{33}S$ slope = 0.9)[50] and Felsic volcanic array (FVA) ($\delta^{34}S$−$\Delta^{33}S$ slope = −0.45).[24] The $\Delta^{33}S$ and $\delta^{34}S$ values of Beijing $PM_{2.5}$ in spring, summer and autumn (−0.011 ‰ ≤ $\Delta^{33}S$ ≤ 0.480 ‰ and 3.3 ‰ ≤ $\delta^{34}S$ ≤ 7.4 ‰) are within the range reported in Xianghe aerosols (−0.056 ‰ ≤ $\Delta^{33}S$ ≤ 0.525 ‰ and 1.4 ‰ ≤ $\delta^{34}S$ ≤ 9.2 ‰), which were collected in spring and summer (Figure 4B),[26] reflecting similar processes of sulfate formation. However, strongly negative $\Delta^{33}S$ values of $PM_{2.5}$ in winter have not been reported before and are distinctly different from California aerosols collected in winter.[25]

Mass independent isotopic compositions can be caused by several factors, including nuclear field shift effects, photochemical reaction and surface reaction effects, etc.[25,26,31] However, nuclear field shift effects, surface reaction effects, symmetry and magnetic isotope effects have been excluded for mass-independent fractionation of sulfur isotopes (S-MIF).[26] This leaves SO_2 photolysis at short wavelengths as the most

DOI: 10.1021/acs.est.7b00280
Environ. Sci. Technol. 2017, 51, 7794−7803

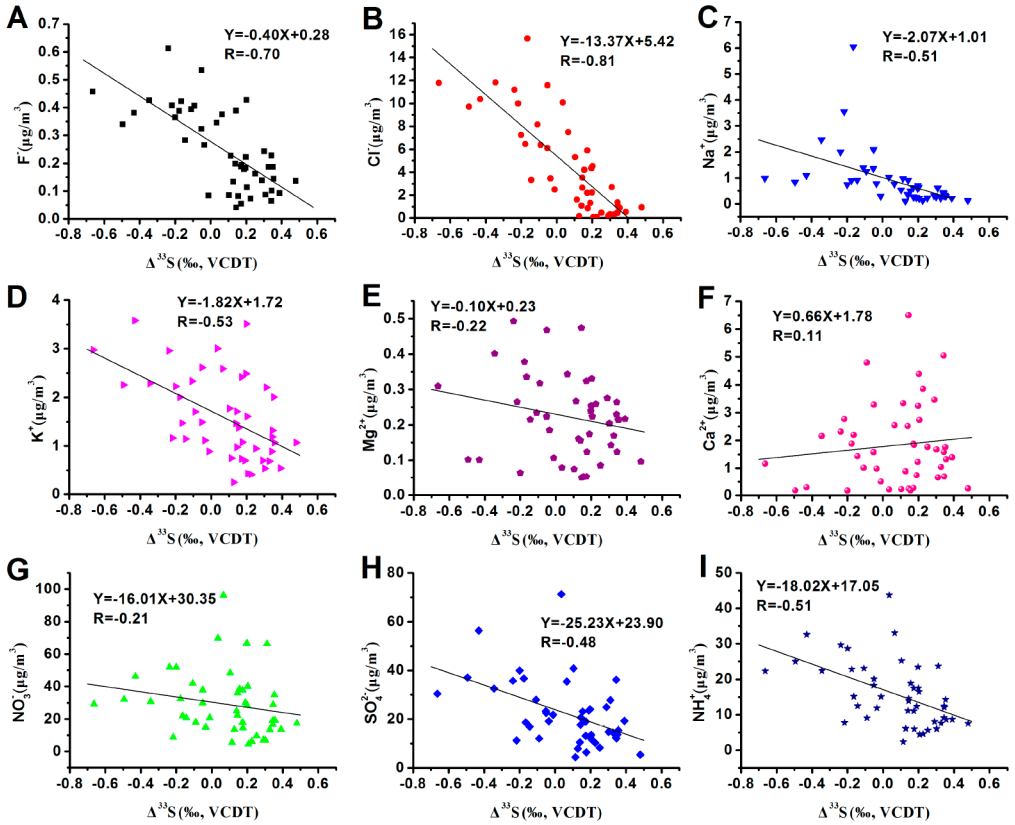

Figure 5. Correlations between $\Delta^{33}S$ and water-soluble ions in Beijing $PM_{2.5}$. (A) F^- and $\Delta^{33}S$; (B) Cl^- and $\Delta^{33}S$; (C) Na^+ and $\Delta^{33}S$; (D) K^+ and $\Delta^{33}S$; (E) Mg^{2+} and $\Delta^{33}S$; (F) Ca^{2+} and $\Delta^{33}S$; (G) NO_3^- and $\Delta^{33}S$; (H) SO_4^{2-} and $\Delta^{33}S$; (I) NH_4^+ and $\Delta^{33}S$.

likely candidate for S-MIF production.[29−31,51] Experimental studies have shown that SO_2 photolysis in the wavelength region of 190−220 nm can produce large S-MIF signatures influenced by gas pressure and gas composition.[29,30]

Different causes responsible for sizable S-MIF effects related to SO_2 photolysis have been discussed: the spectrum of radiation available for photolysis (mutual shielding and self-shielding); isotopologue-specific probability of photoexcitation prior to dissociation; kinetic isotope effects related to state-to-state transitions for isotopologues.[29,30,50] Farquhar et al.[29] suggested the S-MIF signatures to result from simple photodissociation, which did not consider the effect of self-shielding. Recent experimental studies, however, have shown that SO_2 photolysis with self-shielding produces elemental sulfur with large S-MIF signals (positive $\Delta^{33}S$ values) and a $\delta^{34}S$-$\Delta^{33}S$ slope of 0.086 ± 0.035.[50] This would be fully consistent with sulfur isotope anomalies ($\Delta^{33}S$) observed for sulfate in Beijing $PM_{2.5}$ in spring, summer, and autumn (Figure 4A). However, SO_2 photolysis can not occur in the troposphere because the radiation in the 190−220 nm region is absorbed by O_2 and O_3 in the modern atmosphere.[29,31] In contrast, respective processes would be possible at an altitude of 20−25 km, that is, in the stratosphere.[31] Thus, we propose that the positive $\Delta^{33}S$ values measured in the Beijing $PM_{2.5}$ sulfate may reflect SO_2 photolysis with self-shielding, possibly due to an air mass transport between the troposphere and the stratosphere.[25] Ono et al. reported that SO_2 photolysis with self-shielding can produce a $\Delta^{33}S$ value of 11.79‰ and a $\delta^{34}S$ value of 118.67‰ under the condition of pSO_2 = 0.89mbar pN_2 = 0.22 bar, and a flow rate = 25 sccm.[50] Based on these values and the maximal $\Delta^{33}S$ value of 0.480‰ observed in $PM_{2.5}$, it is estimated that at most 1.57% of the sulfate in $PM_{2.5}$ can originate from the stratosphere, which may cause an increase of less than 1.86‰ in the $\delta^{34}S$ value of sulfate in $PM_{2.5}$.

A different source of S-MIF is SO_2 photoexcitation in the 250−320 nm region, recently proposed based on numerical modeling.[52] The model results of SO_2 photoexcitation agree well with S-MIF signatures of volcanic sulfate preserved in polar ice and snowpacks.[52] However, respective photochemical experiments, that is, SO_2 photoexcitation in the 250−330 nm, resulted in sulfate lacking S-MIF and elemental sulfur characterized by positive $\Delta^{36}S/\Delta^{33}S$ ratios.[51] Considering the negative $\Delta^{36}S/\Delta^{33}S$ ratios observed in modern sulfate aerosols,[25,26] it may indicate that SO_2 photoexcitation is not a likely source for the sulfur isotope anomalies observed in this study.

Negative $\Delta^{33}S$ values of sulfate in Beijing $PM_{2.5}$ have been measured for aerosol samples collected in winter (Figure 4B). This is different from winter aerosols in Bakersfield, California (0.00‰ < $\Delta^{33}S$ < 0.47‰; mean = 0.203 ± 0.154‰, n = 20) reported by Romero and Thiemens.[25] With somewhat comparable climatic conditions for sampling (both in winter), the observed difference in $\Delta^{33}S$ values could be related to different sulfate sources. While $\delta^{34}S$ values between +3.05 and +12.32‰ for Bakersfield aerosols suggest a mixture between seawater and anthropogenic sulfate,[25] $\delta^{34}S$ values for sulfate in Beijing $PM_{2.5}$ indicate a mixture of sulfate from oil combustion, coal combustion, and biogenic origin.

$\Delta^{33}S$ values measured for sulfate in Beijing $PM_{2.5}$ aerosol display significant negative correlations with water-soluble ions (F^-, Cl^-, Na^+, K^+, and NH_4^+) (Figure 5). In winter, the increase in concentrations of F^-, Cl^-, Na^+, and NH_4^+ is

DOI: 10.1021/acs.est.7b00280
Environ. Sci. Technol. 2017, 51, 7794−7803

associated with the increase in coal consumption.[5,53,54] During combustion, volatile elements (F^-, Cl^-, and Na^+, etc.) are released via flue gases through complex reactions.[53,55] For instance, chlorine in coal is emitted into the atmosphere as HCl, NaCl, KCl, and CH_3Cl, etc.[55,56] Recent $\delta^{15}N$ results indicate that most of NH_3 during haze days in Beijing is derived from fossil fuel combustion.[5] Therefore, the negative correlations between $\Delta^{33}S$ values and water-soluble ions suggest that negative $\Delta^{33}S$ signatures are possibly related to coal combustion.

Laboratory studies reveal that a negative $\Delta^{33}S$ signature can be attributed to primary sulfate from combustion of fossil fuel and biomass materials ($\Delta^{33}S$ = −0.227‰ to 0.031‰, n = 8),[27,57] suggesting that a $\Delta^{33}S$ change can occur during these combustion processes. A distinct sulfur isotopic fractionation would be transferred to SO_2 emitted from fossil fuel combustion. The oxygen isotopic evidence shows that sulfate in Beijing $PM_{2.5}$ mainly originates from the oxidation of SO_2, indicating that the negative $\Delta^{33}S$ signature in $PM_{2.5}$ was mainly linked to secondary sulfate. There is a discrepancy between the experimental result that negative $\Delta^{33}S$ values are related with primary sulfate and the oxygen isotopic evidence suggesting that the negative values observed in $PM_{2.5}$ are associated with secondary sulfate. This discrepancy need to be further investigated with combustion experiments, in order to determine whether such effects can be reproduced and to identify factors affecting the fractionation of sulfur isotopes.

In North China, sulfur emission from coal combustion shows an increase in winter because of domestic heating, which may lead to a change in $\Delta^{33}S$ values of sulfate in $PM_{2.5}$. Sulfate, pyrite, and organic sulfur are three main forms of sulfur in coal. Most of the pyrite and the organic sulfur will be converted to SO_2 during coal combustion. In flue gas, some of SO_2 may be captured by minor cations (Ca^{2+}, K^+, Na^+, Fe^{3+}, etc.) in the coal, which is affected by temperature and sulfur content.[56] It is indicated that the magnitude in sulfur isotopic fractionation during coal combustion is dependent on combustion conditions. In fact, incomplete combustion often occurs in residential stoves during the heating period, and this could result in a distinct sulfur isotopic fractionation. Furthermore, residential stoves used for heating in rural areas of North China are different from industrial boilers, because the former have significantly higher emissions of $PM_{2.5}$ than the latter (almost 100times).[58] Combined with a distinct sulfur isotopic fractionation, this distinct sulfur isotope signature would be transferred into the atmosphere. However, limited experimental data display that $\Delta^{33}S$ values of sulfate formed during combustion range from −0.227‰ to 0.031‰ (n = 8),[27,57] which cannot explain the negative $\Delta^{33}S$ anomalies (−0.664‰ < $\Delta^{33}S$ ← 0.300‰) of $PM_{2.5}$ sulfate in winter. Therefore, the negative $\Delta^{33}S$ values of $PM_{2.5}$ sulfate observed in winter may be linked to the incomplete combustion of residential stoves during the heating season and other factors.

Negative $\Delta^{33}S$ anomalies can be caused by carbonyl sulfide (OCS) shielding.[59] However, in the present-day oxygen rich atmosphere, the content of COS in the troposphere is ∼500 parts per trillion,[60] implying that the contribution of COS to S-MIF may be less significant. The absence of a sulfur isotope anomaly ($\Delta^{33}S$ = ±0.2‰) in younger sediments[20] indicates that sulfur isotopic equilibrium exists in modern environments. Considering an isotope mass balance, a mass-weighted positive $\Delta^{33}S$ signal formed in atmosphere would be balanced with a mass-weighted negative $\Delta^{33}S$ signal.[23] Respective $\Delta^{33}S$ values for sulfate in $PM_{2.5}$ from Beijing during different seasons seem to balance each other around an annual arithmetic mean value of 0.075 ± 0.253‰ (n = 48), that is, showing an apparent solely mass dependent sulfur isotopic fractionation for aerosol sulfate. We propose that such an isotope mass balance explains the $\Delta^{33}S$ anomalies observed in modern aerosols and the observed lack of S-MIF in modern sediments.

Some special atmospheric conditions in winter may lead to a negative $\Delta^{33}S$ signature observed in Beijing $PM_{2.5}$. The $PM_{2.5}$ concentration is high during winter sampling period. Besides emission sources, stable synoptic meteorological conditions play an important role in the formation of high $PM_{2.5}$ concentration.[61] It has been reported that a temperature inversion at an altitude of around 1−2 km above the surface was often observed in Beijing winter,[62] which prevented air mass from vertical transport. This may suggest that the contribution of sulfate from the stratosphere to sulfate in $PM_{2.5}$ decreased in winter, resulting in $PM_{2.5}$ sulfate showing almost no contribution of positive $\Delta^{33}S$ anomalies from stratospheric sulfate.

■ ASSOCIATED CONTENT

Supporting Information

The Supporting Information is available free of charge on the ACS Publications website at DOI: 10.1021/acs.est.7b00280.

Meteorological parameters during $PM_{2.5}$ sampling, back trajectories of air masses for four events, and concentrations of water-soluble inorganic ions and sulfur isotopes of sulfate in $PM_{2.5}$ (PDF)

■ AUTHOR INFORMATION

Corresponding Author

*E-mail: guoqj@igsnrr.ac.cn. Fax: +86-01-64889455. Tel: +86-10-64889455.

ORCID

Xiaokun Han: 0000-0002-3805-3592

Qingjun Guo: 0000-0003-1538-1339

Author Contributions

Q.G. contributed to the conception of the study, performed the data analyses and wrote the manuscript; X.H. performed the data analyses and wrote the manuscript; Q.G., H.S., C.L., J.H., Z.G., and M.P. helped to perform the analyses and contributed to the manuscript with constructive discussions; R.W. and L.T. performed the experiments; and J.K. collected the samples.

Notes

The authors declare no competing financial interest.

■ ACKNOWLEDGMENTS

This work was funded by NSFC (Nos. 41625006 and 4151101008), Project of Chinese Academy of Sciences (No. XDB15020401), the Sino-German Center (No. GZ1055), and the Feature Institute Program of the Chinese Academy of Sciences (Comprehensive Technical Scheme and Integrated Demonstration for Remediation of Soil and Groundwater in Typical Area).

■ REFERENCES

(1) Chan, C. K.; Yao, X. Air pollution in mega cities in China. *Atmos. Environ.* **2008**, *42*, 1−42.

(2) Huang, R. J.; Zhang, Y.; Bozzetti, C.; Ho, K.-F.; Cao, J.-J.; Han, Y.; Daellenbach, K. R.; Slowik, J. G.; Platt, S. M.; Canonaco, F.; Zotter,

DOI: 10.1021/acs.est.7b00280
Environ. Sci. Technol. 2017, 51, 7794−7803

P.; Wolf, R.; Pieber, S. M.; Bruns, E. A.; Crippa, M.; Ciarelli, G.; Piazzalunga, A.; Schwikowski, M.; Abbaszade, G.; SchnelleKreis, J.; Zimmermann, R.; An, Z.; Szidat, S.; Baltensperger, U.; Haddad, I. E.; Prevot, A. S. H. High secondary aerosol contribution to particulate pollution during haze events in China. *Nature* **2014**, *514*, 218−222.

(3) Li, M.; Zhang, L. Haze in China: Current and future challenges. *Environ. Pollut.* **2014**, *189*, 85−86.

(4) Andersson, A.; Deng, J.; Du, K.; Zheng, M.; Yan, C.; Sköld, M.; Gustafsson, O. Regionally-varying combustion sources of the January 2013 severe haze events over eastern China. *Environ. Sci. Technol.* **2015**, *49* (4), 2038−2043.

(5) Pan, Y.; Tian, S.; Liu, D.; Fang, Y.; Zhu, X.; Zhang, Q.; Zheng, B.; Michalski, G.; Wang, Y. Fossil fuel combustion-related emissions dominate atmospheric ammonia sources during severe haze episodes: Evidence from ^{15}N-stable isotope in size-resolved aerosol ammonium. *Environ. Sci. Technol.* **2016**, *50* (15), 8049−8056.

(6) Atkinson, R. W.; Kang, S.; Anderson, H. R.; Mills, I. C.; Walton, H. A. Epidemiological time series studies of $PM_{2.5}$ and daily mortality and hospital admissions: a systematic review and meta-analysis. *Thorax* **2014**, *69*, 660.

(7) Andreae, M. O.; Rosenfeld, D. Aerosol-cloud-precipitation interactions. Part 1. The nature and sources of cloud-active aerosols. *Earth-Sci. Rev.* **2008**, *89*, 13−41.

(8) Guo, S.; Hu, M.; Zamora, M. L.; Peng, J.; Shang, D.; Zheng, J.; Du, Z.; Wu, Z.; Shao, M.; Zeng, L.; Molina, M. J.; Zhang, R. Elucidating severe urban haze formation in China. *Proc. Natl. Acad. Sci. U. S. A.* **2014**, *111*, 17373−17378.

(9) IPCC. *Climate Change 2007: The Physical Science Basis*, Contribution of Working Group 1 to the Fourth Assessment Report of theIntergovernmental Panel on Climate Change; Solomons, S., Qin, D., Manning, M., Chen, Z., Marquis, M., Avery, K. B., Tignor, M., Miller, H. L., Eds.; Cambridge University Press: Cambridge, U.K., 2007.

(10) Mukai, H.; Tanaka, A.; Fujii, T.; Zeng, Y.; Hong, Y.; Tang, J.; Guo, S.; Xue, H.; Sun, Z.; Zhou, J.; Xue, D.; Zhao, J.; Zhai, G.; Gu, J.; Zhai, P. Regional characteristics of sulfur and lead isotope ratios in the atmosphere at several Chinese urban sites. *Environ. Sci. Technol.* **2001**, *35*, 1064−1071.

(11) Norman, A. L.; Anlauf, K.; Hayden, K.; Thompson, B.; Brook, J. R.; Li, S. M.; Bottenheim, J. Aerosol sulphate and its oxidation on the Pacific NW coast: S and O isotopes in $P_{M2.5}$. *Atmos. Environ.* **2006**, *40*, 2676−2689.

(12) Xiao, H. Y.; Wang, Y. L.; Tang, C. G.; Liu, C. Q. Indicating atmospheric sulfur by means of S-isotope in leaves of the plane, osmanthus and camphor trees. *Environ. Pollut.* **2012**, *162*, 80−85.

(13) Han, X.; Guo, Q.; Liu, C.; Fu, P.; Strauss, H.; Yang, J.; Hu, J.; Wei, L.; Ren, H.; Peters, M.; Wei, R.; Tian, L. Using stable isotopes to trace sources and formation processes of sulfate aerosols from Beijing, China. *Sci. Rep.* **2016**, *6*, 29958.

(14) Inomata, Y.; Ohizumi, T.; Take, N.; Sato, K.; Nishikawa, M. Transboundary transport of anthropogenic sulfur in $PM_{2.5}$ at a coastal site in the Sea of Japan as studied by sulfur isotopic ratio measurement. *Sci. Total Environ.* **2016**, *553*, 617−625.

(15) Ohizumi, T.; Take, N.; Inomata, Y.; Yagoh, H.; Endo, T.; Takahashi, M.; Yanahara, K.; Kusakabe, M. Long-term variation of the source of sulfate deposition in a leeward area of Asian continent in view of sulfur isotopic composition. *Atmos. Environ.* **2016**, *140*, 42−51.

(16) Sinha, B. W.; Hoppe, P.; Huth, J.; Foley, S.; Andreae, M. O. Sulfur isotope analyses of individual aerosol particles in the urban aerosol at a central European site (Mainz, Germany). *Atmos. Chem. Phys.* **2008**, *8*, 7217−7238.

(17) Kunasek, S. A.; Alexander, B.; Steig, E. J.; Sofen, E. D.; Jackson, T. L.; Thiemens, M. H.; McConnell, J. R.; Gleason, D. J.; Amos, H. M. Sulfate sources and oxidation chemistry over the past 230 years from sulfur and oxygen isotopes of sulfate in a West Antarctic ice core. *J. Geophys. Res.* **2010**, *115*, D18313.

(18) Harris, E.; Sinha, B.; Hoppe, P.; Ono, S. High-precision measurements of ^{33}S and ^{34}S fractionation during SO_2 oxidation reveal causes of seasonality in SO_2 and sulfate isotopic composition. *Environ. Sci. Technol.* **2013**, *47* (21), 12174−12183.

(19) Farquhar, J.; Bao, H.; Thiemens, M. Atmospheric influence of Earth's earliest sulfur cycle. *Science* **2000**, *289*, 756−758.

(20) Farquhar, J.; Peters, M.; Johnston, D. T.; Strauss, H.; Masterson, A.; Wiechert, U.; Kaufman, A. J. Isotopic evidence for Mesoarchaean anoxia and changing atmospheric sulphur chemistry. *Nature* **2007**, *449*, 706−709.

(21) Muller, É.; Philippot, P.; Rollion-Bard, C.; Cartigny, P. Multiple sulfur-isotope signatures in Archean sulfates and their implications for the chemistry and dynamics of the early atmosphere. *Proc. Natl. Acad. Sci. U. S. A.* **2016**, *113* (27), 7432−7437.

(22) Savarino, J.; Romero, A.; Cole-Dai, J.; Bekki, S.; Thiemens, M. H. UV induced mass-independent sulfur isotope fractionation in stratospheric volcanic sulfate. *Geophys. Res. Lett.* **2003**, *30*, 2131.

(23) Baroni, M.; Thiemens, M. H.; Delmas, R. J.; Savarino, J. Mass-independent sulfur isotopic compositions in stratospheric volcanic eruptions. *Science* **2007**, *315*, 84−87.

(24) Philippot, P.; van Zuilen, M.; Rollion-Bard, C. Variations in atmospheric sulphur chemistry on early Earth linked to volcanic activity. *Nat. Geosci.* **2012**, *5*, 668−674.

(25) Romero, A. B.; Thiemens, M. H. Mass-independent sulfur isotopic compositions in present-day sulfate aerosols. *J. Geophys. Res.* **2003**, *108* (D16), 4524.

(26) Guo, Z.; Li, Z.; Farquhar, J.; Kaufman, A. J.; Wu, N.; Li, C.; Dickerson, R. R.; Wang, P. Identification of sources and formation processes of atmospheric sulfate by sulfur isotope and scanning electron microscope measurements. *J. Geophys. Res.* **2010**, *115*, D00K07.

(27) Shaheen, R.; Abaunza, M. M.; Jackson, T. L.; McCabe, J.; Savarino, J.; Thiemens, M. H. Large sulfur-isotope anomaly in nonvolcanic sulfate aerosol and its implications for the Archean atmosphere. *Proc. Natl. Acad. Sci. U. S. A.* **2014**, *111* (33), 11979−11983.

(28) Guo, Q.; Strauss, H.; Kaufman, A. J.; Schröder, S.; Gutzmer, J.; Wing, B.; Baker, M. A.; Bekker, A.; Kim, S. T.; Jin, Q.; Farquhar, J. Reconstructing Earth's surface oxidation across the Archean-Proterozoic transition. *Geology* **2009**, *37*, 399−402.

(29) Farquhar, J.; Savarino, J.; Airieau, S.; Thiemens, M. H. Observation of wavelength-sensitive mass-independent sulfur isotope effects during SO_2 photolysis: Implications for the early atmosphere. *J. Geophys. Res.* **2001**, *106* (E12), 32829−32839.

(30) Masterson, A. L.; Farquhar, J.; Wing, B. A. Sulfur mass-independent fractionation patterns in the broadband UV photolysis of sulfur dioxide: Pressure and third body effects. *Earth Planet. Sci. Lett.* **2011**, *306*, 253−260.

(31) Whitehill, A. R.; Jiang, B.; Guo, H.; Ono, S. SO_2 photolysis as a source for sulfur mass-independent isotope signatures in stratospehric aerosols. *Atmos. Chem. Phys.* **2015**, *15*, 1843−1864.

(32) Finlayson-Pitts, B. J.; Pitts, J. N. *Chemistry of the Upper and Lower Atmosphere: Theory, Experiments, and Applications*; Academic Press: San Diego, CA, 1999; 969 pp.

(33) Thode, H. G.; Monster, J.; Dunford, H. B. Sulphur isotope geochemistry. *Geochim. Cosmochim. Acta* **1961**, *25* (3), 159−174.

(34) Forrest, J.; Newman, L. Silver-110 microgram sulfate analysis for short time resolution of ambient levels of sulfur aerosol. *Anal. Chem.* **1977**, *49*, 1579−1584.

(35) Hulston, J. R.; Thode, H. G. Variations in the ^{33}S, ^{34}S, and ^{36}S contents of meteorites and their relation to chemical and nuclear effects. *J. Geophys. Res.* **1965**, *70* (14), 3475−3484.

(36) Farquhar, J.; Wing, B. A. Multiple sulfur isotopes and the evolution of the atmosphere. *Earth Planet. Sci. Lett.* **2003**, *213* (1), 1−13.

(37) Stein, A. F.; Draxler, R. R.; Rolph, G. D.; Stunder, B. J. B.; Cohen, M. D.; Ngan, F. NOAA's HYSPLIT atmospheric transport and dispersion modeling system. *Bull. Am. Meteorol. Soc.* **2015**, *96*, 2059−2077.

(38) Patris, N.; Delmas, R.; Legrand, M.; De Angelis, M.; Ferron, F. A.; Stiévenard, M.; Jouzel, J. First sulfur isotope measurements in

DOI: 10.1021/acs.est.7b00280
Environ. Sci. Technol. 2017, 51, 7794−7803

central Greenland ice cores along the preindustrial and industrial periods. *J. Geophys. Res.* **2002**, *107*, ACH-6-1.
(39) Kong, S.; Ji, Y.; Lu, B.; Chen, L.; Han, B.; Li, Z.; Bai, Z. Characterization of PM_{10} source profiles for fugitive dust in Fushun-a city famous for coal. *Atmos. Environ.* **2011**, *45*, 5351−5365.
(40) Zhang, Q.; Shen, Z.; Cao, J.; Ho, K.; Zhang, R.; Bie, Z.; Chang, H.; Liu, S. Chemical profiles of urban fugitive dust over Xi'an in the south margin of the Loess Plateau, China. *Atmos. Pollut. Res.* **2014**, *5*, 421−430.
(41) Maruyama, T.; Ohizumi, T.; Taneoka, Y.; Minami, N.; Fukuzaki, N.; Mukai, H.; Murano, K.; Kusakabe, M. Sulfur isotope ratios of coals and oils used in China and Japan. *Nippon Kagaku Kaishi* **2000**, *1*, 45−51 (in Japanese)..
(42) Nriagu, J. O.; Holdway, D. A.; Coker, R. D. Biogenic sulfur and the acidity of rainfall in remote areas of Canada. *Science* **1987**, *237*, 1189−1192.
(43) Liu, G. S.; Hong, Y. T.; Piao, H. C.; Zeng, Y. Q. Study on sources of sulfur in atmospheric particulate matter with stable isotope method. *China Environ. Sci.* **1996**, *12* (6), 426−429 (in Chinese with English abstract)..
(44) Mast, M. A.; Turk, J. T.; Ingersoll, G. P.; Clow, D. W.; Kester, C. L. Use of stable sulfur isotopes to identify sources of sulfate in Rocky Mountain snowpacks. *Atmos. Environ.* **2001**, *35*, 3303−3313.
(45) Hong, Y.; Zhang, H.; Zhu, Y. Sulfur isotopic characteristics of coal in China and sulfur isotopic fractionation during coal-burning process. *Chin. J. Geochem.* **1993**, *12* (1), 51−59.
(46) Novák, M.; Jačková, I.; Prechová, E. Temporal trends in the isotope signature of air-borne sulfur in Central Europe. *Environ. Sci. Technol.* **2001**, *35* (2), 255−260.
(47) Holt, B. D. The oxygen isotope analysis of sulphur and oxygen isotopes: oxygen isotopes. In *Stable Isotopes: Natural and Anthropogenic Sulphur in the Environment. SCOPE 43*; Krouse, H. R., Grinenko, V. A., Eds.; Wiley: New York, 1991; pp 55−64.
(48) Wen, X. F.; Zhang, S. C.; Sun, X. M.; Yu, G. R.; Lee, X. Water vapor and precipitation isotope ratios in Beijing, China. *J. Geophys. Res.* **2010**, *115*, D01103.
(49) Guo, Z.; Wu, M.; Liu, F.; Wei, Y.; Li, D. Multiple sulfur and oxygen isotope compositions in Beijing aerosol. *Sci. China: Earth Sci.* **2014**, *57* (11), 2671−2675.
(50) Ono, S.; Whitehill, A. R.; Lyons, J. R. Contribution of isotopologue self-shielding to sulfur mass-independent fractionation during sulfur dioxide photolysis. *J. Geophys. Res.* **2013**, *118*, 2444−2454.
(51) Whitehill, A. R.; Ono, S. Excitation band dependence of sulfur isotope mass-independent fractionation during photochemistry of sulfur dioxide using broadband light sources. *Geochim. Cosmochim. Acta* **2012**, *94*, 238−253.
(52) Hattori, S.; Schmidt, J. A.; Johnson, M. S.; Danielache, S. O.; Yamada, A.; Ueno, Y.; Yoshida, N. SO_2 photoexcitation mechanism links mass-independent sulfur isotopic fractionation in cryospheric sulfate to climate impacting volcanism. *Proc. Natl. Acad. Sci. U. S. A.* **2013**, *110* (44), 17656−17661.
(53) Clarke, L. B. The fate of trace elements during coal combustion and gasification: an overview. *Fuel* **1993**, *72*, 731−736.
(54) Wang, Y.; Zhuang, G.; Tang, A.; Yuan, H.; Sun, Y.; Chen, S.; Zheng, A. The ion chemistry and the source of $PM_{2.5}$ aerosol in Beijing. *Atmos. Environ.* **2005**, *39* (21), 3771−3784.
(55) McCulloch, A.; Aucott, M. L.; Benkovitz, C. M.; Graedel, T. E.; Kleiman, G.; Midgley, P. M.; Li, Y. F. Global emissions of hydrogen chloride and chloromethane from coal combustion, incineration and industrial activities: Reactive Chlorine Emissions Inventory. *J. Geophys. Res.* **1999**, *104* (D7), 8391−8403.
(56) Yan, R.; Gauthier, D.; Flamant, G.; Badie, J. M. Thermodynamic study of the behaviour of minor coal elements and their affinities to sulphur during coal combustion. *Fuel* **1999**, *78*, 1817−1829.
(57) Lee, C. W.; Savarino, J. H.; Cachier, H.; Thiemens, M. H. Sulfur (^{32}S, ^{33}S, ^{34}S, ^{36}S) and oxygen (^{16}O, ^{17}O, ^{18}O) isotopic ratios of primary sulfate produced from combustion processes. *Tellus, Ser. B* **2002**, *54* (3), 193−200.
(58) Zhang, Y.; Schauer, J. J.; Zhang, Y.; Zeng, L.; Wei, Y.; Liu, Y.; Shao, M. Characteristics of particulate carbon emissions from real-world Chinese coal combustion. *Environ. Sci. Technol.* **2008**, *42*, 5068−5073.
(59) Ueno, Y.; Johnson, M. S.; Danielache, S. O.; Eskebjerg, C.; Pandey, A.; Yoshida, N. Geological sulfur isotopes indicate elevated OCS in the Archean atmosphere, solving faint young sun paradox. *Proc. Natl. Acad. Sci. U. S. A.* **2009**, *106* (35), 14784−14789.
(60) Chin, M.; Davis, D. D. A reanalysis of carbonyl sulfide as a source of stratospheric background sulfur aerosol. *J. Geophys. Res.* **1995**, *100* (D5), 8993−9005.
(61) Zheng, G. J.; Duan, F. K.; Su, H.; Ma, Y. L.; Cheng, Y.; Zheng, B.; Zhang, Q.; Huang, T.; Kimoto, T.; Chang, D.; Pöschl, U.; Cheng, Y. F.; He, K. B. Exploring the severe winter haze in Beijing: the impact of synoptic weather, regional transport and heterogeneous reactions. *Atmos. Chem. Phys.* **2015**, *15* (6), 2969−2983.
(62) Li, J.; Du, H.; Wang, Z.; Sun, Y.; Yang, W.; Li, J.; Tang, X.; Fu, P. Rapid formation of a severe regional winter haze episode over a megacity cluster on the North China Plain. *Environ. Pollut.* **2017**, *223*, 605−615.
(63) Guo, Q.; Strauss, H.; Chen, T. B.; Zhu, G.; Yang, J.; Yang, J.; Lei, M.; Zhou, X.; Peters, M.; Xie, Y.; Zhang, H.; Wei, R.; Wang, C. Tracing the source of Beijing soil organic carbon: a carbon isotope approach. *Environ. Pollut.* **2013**, *176*, 208−214.
(64) Meng, Y.; Tang, C. Study on the trend of population spatial distribution in Beijing since the Reform and Opening-up: Based on analyzing the data of four population census from 1982 to 2010. *China Population, Resources and Environment* **2015**, *25* (3), 135−142 (in Chinese with English abstract).

DOI: 10.1021/acs.est.7b00280
Environ. Sci. Technol. 2017, 51, 7794−7803